

A transmission electron microscopy investigation of SiC films grown on Si(111) substrates by solid-source molecular beam epitaxy

U. Kaiser^{a)}

Institut für Festkörperphysik, Friedrich-Schiller-Universität Jena, Max-Wien-Platz 1, D-07743 Jena, Germany

S. B. Newcomb and W. M. Stobbs^{b)}

Department of Materials Science and Metallurgy, University of Cambridge, Pembroke Street, Cambridge, CB2 3QZ, United Kingdom

M. Adamik

Research Institute for Technical Physics, H-1325, P.O. Box 76, Budapest, Hungary

A. Fissel and W. Richter

Institut für Festkörperphysik, Friedrich-Schiller-Universität Jena, Max-Wien-Platz 1, D-07743 Jena, Germany

(Received 4 August 1997; accepted 10 June 1998)

The effects of different growth parameters on the microstructure of the SiC films formed during simultaneous two-source molecular-beam-epitaxial (MBE) deposition have been investigated. Substrate temperatures as low as 750–900 °C have been used. The relationship between a number of different growth morphologies and deposition conditions has been established. The formation of single-crystal 3C films has been found to occur at low growth rates but within a limited Si:C adatom ratio. A combination of transmission electron microscopy (TEM) and atomic force microscopy (AFM) has been used to examine the different films, and the results of these investigations are described.

I. INTRODUCTION

In recent years there has been a trend toward the use of solid-source molecular-beam epitaxy (MBE)^{1–4} rather than chemical vapor deposition (CVD)^{5–7} to deposit epitaxial SiC layers on Si substrates. The origin of this trend mainly derives from the fact that the former method necessitates having a high substrate temperature which can lead to the subsequent development of rough and defective interfaces. The importance of growing SiC films at relatively low temperatures is emphasized still further by the fact that there is an increasing need for films with sharp doping profiles. However, at temperatures lower than 1000 °C, decomposition of the gas-phase reactants leads to the production of high quantities of atomic hydrogen which is adsorbed onto the growing SiC surface.⁸ Since the desorption rate of hydrogen is very low, extremely low growth rates have to be used to overcome the problem of hydrogen adsorption. For this reason solid-source MBE has attracted considerable interest as a method of growing SiC films. Although Kaneda *et al.*^{4,5} have obtained stoichiometric SiC films on Si(111) and SiC(0001) substrates, this has been achieved only with substrate temperatures above 1100 °C, and it has been concluded that for

stoichiometric films the adatom ratio of Si:C has to be exactly 1:1.^{6,9}

We have attempted to grow SiC films on (111)Si using solid-source MBE at temperatures below 900 °C and examined the degree to which a reduction in the Si:C adatom ratio can control the formation of epitaxial stoichiometric single phase films. Here we describe an investigation of the influence of a range of growth parameters, including substrate temperature and growth rate, on the quality of the SiC overlayers, as examined using both transmission electron microscopy (TEM) and atomic force microscopy (AFM). Further comparisons have been made for films grown under the above conditions and those formed in ultrahigh vacuum either by carbonization or by alternate deposition from two solid sources.

II. EXPERIMENTAL

SiC films were grown by solid-source MBE (RIBER MBE system) at 750, 800, 850, and 900 °C at growth rates which varied between 0.6 and 6.0 nm/min under a flux rate ratio (adatom ratio) of Si/C of between 0.9 and 1.25. Three growth regimes were used: simultaneous deposition from two sources, alternate deposition, and carbonization of the Si surface, as described more fully elsewhere.^{7,10–14} For comparison, SiC layers were deposited at 10^{−5} Torr on a substrate held at 830 °C.^{12,13}

^{a)}Address correspondence to this author.

^{b)}Deceased.

In all cases, the growth was characterized *in situ* using reflection high energy electron diffraction (RHEED). The surface topography and roughness of the different films were investigated by AFM under ambient conditions in contact and tapping modes. The films were prepared for examination both in plan-view and in cross section using standard techniques and investigated using a JEOL 2000FX, TEM.

III. RESULTS AND DISCUSSION

A. Structure of carbonized films

The morphology of the SiC films formed by ultrahigh vacuum carbonization on a Si substrate held at 750 °C is shown in the bright-field micrographs in Figs. 1(a) and 1(b). The grain size of the film is typically 120 nm and the SiC is both highly faulted and faceted, particularly at the upper surface where the rms roughness for an area of 500×500 nm, as shown in Fig. 2(a), was found to be 8 nm. This value fell to 5 nm when the substrate temperature was increased to 800 °C. The grains are generally highly textured and show a $[1\bar{1}0]\text{SiC} // [1\bar{1}0]\text{Si}$ orientation, but they were also twisted in the $[111]$ direction [see inset diffraction pattern in Fig. 1(a), obtained at $[\bar{1}\bar{1}2]$ zone of Si]. Laterally extended voids were found in the Si immediately beneath the film although the SiC tended to bridge these voids, as is particularly apparent in Fig. 1(b) for the void arrowed at V. The high volume fraction of voids found in the film described here may be seen from the optical Normarski micrograph shown in Fig. 2(b) which also demonstrates the triangular shape of the voids.

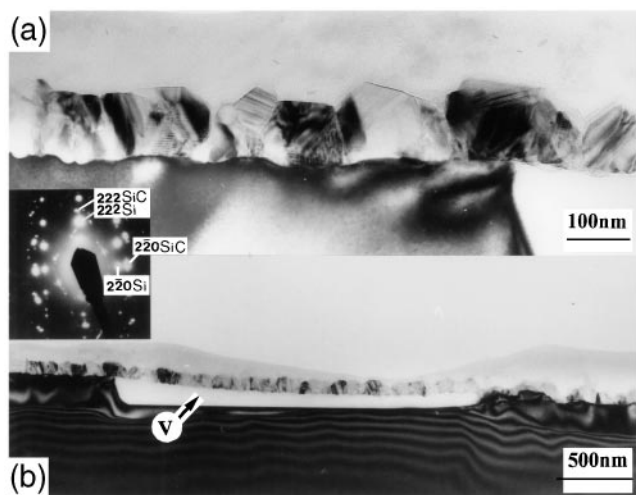


FIG. 1. Cross-sectional, bright-field TEM micrographs of the SiC layer grown by deposition of C at 750 °C showing (a) the wavy structure of the SiC/Si interface and the faceted structure of the SiC surface, and (b) extended void formation, as at V, in the substrate beneath the SiC layer. The inset diffraction pattern, obtained at $[112]$ zone of Si, demonstrates the textured nature of the SiC.

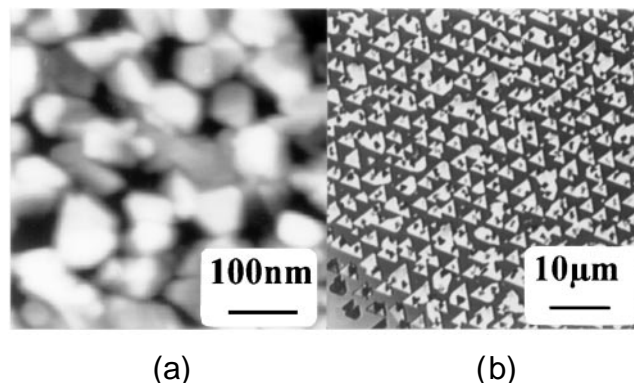


FIG. 2. Plan-view (a) AFM and (b) Normarski micrographs of the film shown in Fig. 1.

B. Film structure at high growth rates (>2 nm/min) and low substrate temperatures (750 °C)

We now examine the effect of forming the film under the same growth conditions but depositing simultaneously from two solid sources. Figure 3 shows the morphology of the MBE film in dark field. It is immediately apparent that the SiC is rather more columnar than was the case when it was formed by carbonization, and it exhibits a rather defective interface with the Si substrate as well as a rough upper surface. The surface roughness was again determined by AFM for an area of 500×500 nm and found to be 11 nm (see Table I, specimen 1), which is somewhat coarser than the 8 nm observed previously. The SiC showed a weak orientation relationship with the underlying Si. It is noted that isolated regions of Si (twinned Si, or single crystal Si in substrate orientation) were observed within the films, and examples of three regions which exhibit twinning are marked in Figs. 3(a) and 3(b). The position of the Si buffer layer interface with the original substrate is easily identified by the way in which it is decorated with a number of defects and an inclined dislocation originating from this interface is labeled D in Fig. 3(b). Furthermore, the lower part of the Si buffer layer is characterized by horizontally layered porosity, as arrowed at P in Fig. 3(a). Although none of the laterally extended voids, which were previously observed, were seen here, the diffusion of Si through porous defects has clearly been initiated, as has also been described elsewhere.¹⁵ There are vertically strained regions in the buffer layer and their width is variable but approximately 15 nm, as indicated. The strained regions bear some relation to the diameters of the 15 nm columnar grains, although it is noted that there are regions of the buffer layer which are strained but above which the SiC is not columnar. Plan-view examination of the SiC overlayer confirmed these observations although a number of regions were found where the grain size was somewhat finer than

TABLE I. Growth parameters and some results for the SiC films formed on (111) Si. The rms roughnesses were determined in precipitate-free $5 \times 5 \mu\text{m}$ areas using AFM.

Specimen	1	2	3	4	5	6	7
Substrate temperature (°C)	750	830	800	850	800, 850	850	900
Growth rate (nm/min)	6	6	2	2	2	0.6	0.6
Flux ratio Si/C	1	ca. 1	1	1.05	1.05	1.1	0.95–1.01 1.03–1.05 1.20–1.25
rms roughness (nm)	11	15	8.5	4	6	3	2.5 1.2 2.8
Microstructure	columnar	columnar	columnar	columnar	columnar	single crystal	single crystal
Average SiC grain size (nm)	10	70	15	40	60
Orientation of the SiC layer to the Si substrate (SiC//Si)	weak [112]// [112]	weak [110]// [110]	strong [112]// [112] and [110]// [110]	strong [112]// [112] and [110]// [110]	strong [112]// [112] and [110]// [110]	epitaxial 3C	epitaxial 3C
Vacuum	UHV	HV	UHV	UHV	UHV	UHV	UHV

in the cross-sectional micrographs. These results further emphasize the roughness of the upper surface interface and the high local misorientations.

C. Film structure at medium growth rate, higher substrate temperatures, and different adatom ratios

The interactive influence of different growth parameters, namely substrate temperature, growth rate, and adatom Si:C ratio, is now described for the MBE deposition. The growth conditions and the resulting features of the film (e.g., rms roughness, microstructure, average grain size, and orientation relation with the Si substrate) are compared in Table I.

Initially, we can note by comparison with the specimens described in Sec. III.B (specimen 1) that simply increasing the substrate temperature (to 830 °C), and decreasing the vacuum, or the same growth rate and adatom ratio (specimen 2, Table I), resulted in void formation as well as in a higher mean SiC grain size (70 nm) and surface roughness (15 nm). The effects of further changes to the growth parameters were investigated by growing films at 800 °C at the same adatom ratio of 1:1 but at a lower growth rate (2 nm/min; specimen 3, Table I). It is noted that by comparison with specimen 2 the relatively low growth rate has resulted in a reduced surface roughness while the SiC grain size is intermediate between that found at 750 and 830 °C. Voids were not, however, seen in the Si beneath the SiC film.

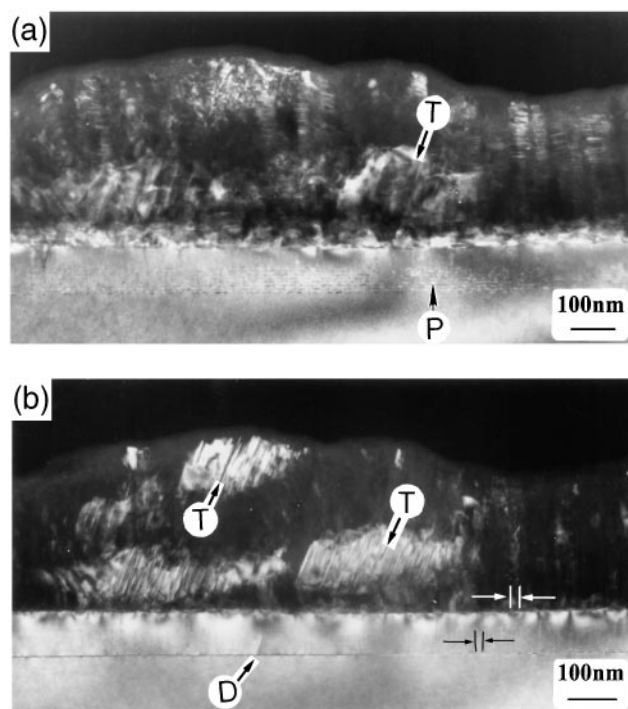


FIG. 3. (a,b) Dark-field TEM micrographs of cross sections of the SiC film formed at 750 °C with a Si:C adatom ratio of 1:1. The buffer layer found beneath the SiC contains pores (as at P) and inclined dislocation (as at D). The SiC is twinned (as at T) and the similarity between the 15 nm width of the columnar SiC grains and the strained regions in the buffer layer is indicated by the marks.

The effect of growing the SiC layer under Si-stabilized conditions and at a Si:C adatom ratio of 1.05 but at 850 °C was investigated (specimen 4, Table I). We now find, not unreasonably, that the grain size of the SiC is coarser than for specimen 3 and that the surface roughness is marginally lower. Figure 4(a) shows a dark-field micrograph of the film and the Si immediately beneath it and it is clear that the interface between them

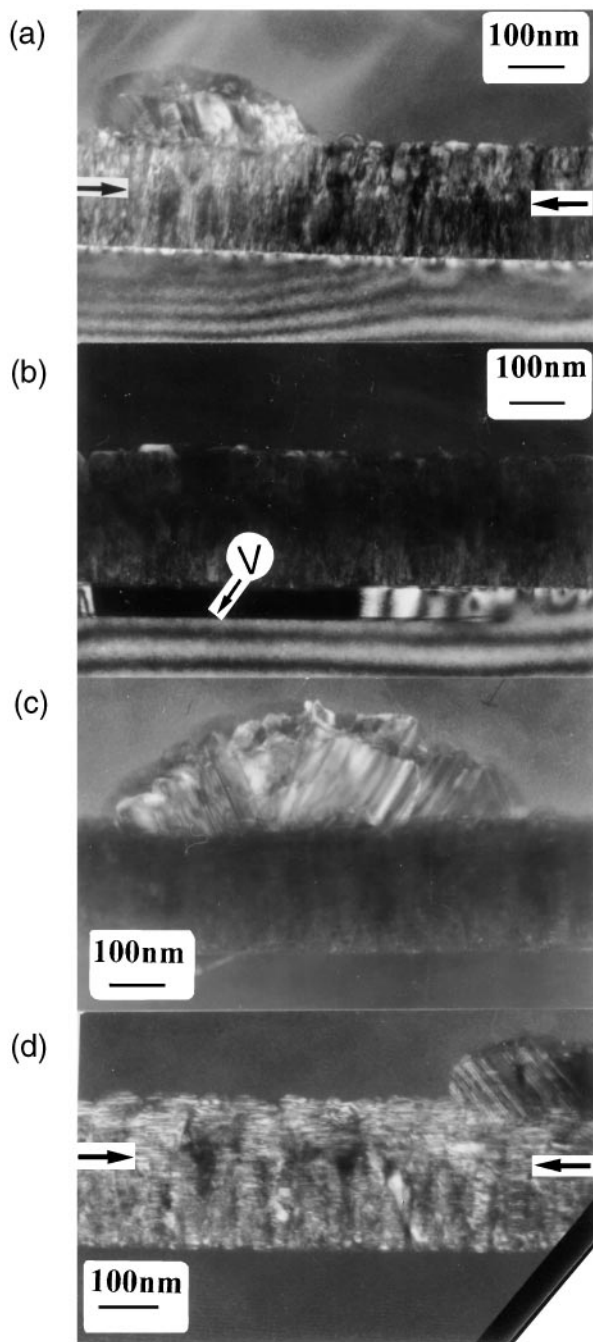


FIG. 4. (a–d) Dark-field micrographs of the SiC formed at 850 °C with a Si:C adatom ratio of 1:1.05. Diffuse boundaries in the film are arrowed in (a) and (d). In (b) voids in the substrate are marked at V.

is strained. We can also see that the upper surface of the film is decorated by a number of isolated islands. These were found to be Si and typically extended some 100–300 nm above the surface of the film. Examples of Si islands are shown in Figs. 4(a), 4(c), and 4(d). We can see that they are generally quite coarse grained and highly twinned although the upper surfaces tend to contain much finer grains. Interestingly, we also find the same type of laterally extended voids as marked in Fig. 4(b) that were observed in the carbonization specimen (see Fig. 1). Although there was no apparent relationship between the observation of these voids and the Si islands, this does not of course indicate that the formation processes are not related. It is also noted that the SiC layer exhibits a diffuse boundary within it and this lies some 150 nm from the upper interface of the Si, as arrowed in Figs. 4(a) and 4(d). This boundary is not, however, obviously associated with any change in grain size of the SiC, but it may be that we are seeing a change in stacking type for the carbide, as perhaps determined by a change in the Si content of the film.

We can now begin to see the way in which the different growth parameters influence the microstructure of the SiC films. At this point, the effects of increasing the growth temperature from 800 to 850 °C after the nucleation of the initial layer were investigated for the same flux rate ratio as before (specimen 5, Table I). These conditions should increase the nucleation density at the beginning of growth, and therefore the problems of high interface roughness should be reduced. Figure 5 shows the morphology of the films formed under these conditions from which we can see that the growth of the film has been bimodal. Extended hillock formation has taken place. Most of the hillocks consist of large faulted cubic SiC grains as well as crystalline Si. These regions of locally accelerated hillock growth are clearly associated with some degree of void formation in the underlying SiC [see Fig. 5(b)]. The second part of the film consists of SiC grains which are highly oriented with respect to the Si substrate. An increase in grain size is seen (see Table I). Plan-view examination showed that the columns are highly faceted and have a hexagonal format with surface normals of $(112)_{\text{Si}}$, as shown in Fig. 5(c). The SiC columns themselves were found to be separated by irregular layers of amorphous material. Figure 6(a) shows a high-resolution TEM image of a part of the overlayer where these amorphous layers are particularly apparent (as arrowed). The amorphous material has also been examined using energy loss imaging techniques, and it was found that there is further evidence for C being present at the vertical SiC interfaces as discussed elsewhere.¹⁶ It is noted, however, that no crystalline graphite precipitates have been observed at the SiC grain boundaries as has been reported by Wahab *et al.*¹⁷ for SiC films grown on Si

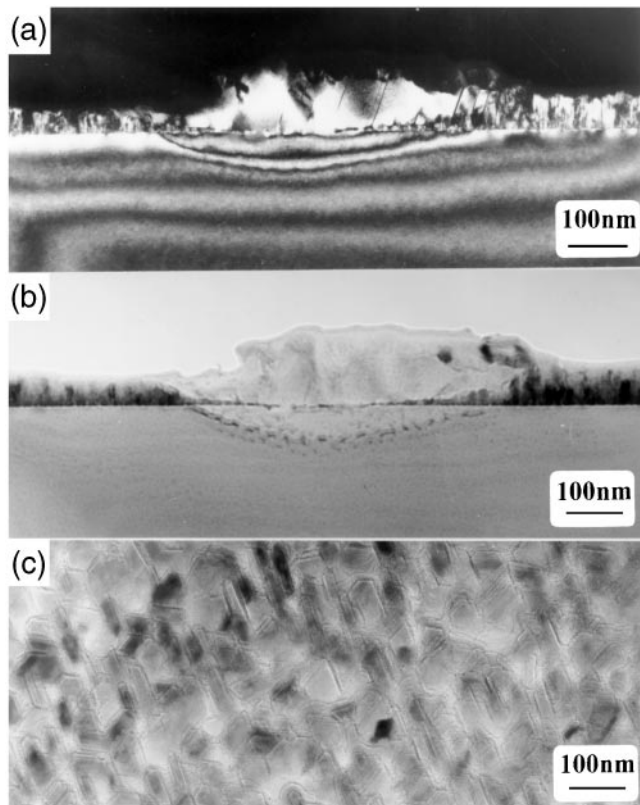


FIG. 5. The microstructure of specimen 5 (see Table I) showing (a) dark- and (b) bright-field cross-sectional and (c) bright-field plan-view micrographs. The bright-field micrograph in (c) was taken in an underfocus condition using the Fresnel contrast to enhance the visibility of the hexagonal faceted grains.

by magnetron sputtering. A higher magnification image of the upper part of the film is shown in Fig. 6(b). We can see the hexagonal polytype (preferentially 4H) although it is noted that the lower part of the film is more typically cubic. The angle between [0001] directions of two columnar interfaces is about 1° .

Growing the initial layer (2 nm) at 850 °C by the alternating supply of Si and C, followed by annealing at the same temperature for 1 h and then depositing simultaneously from both of the sources at the same growth rate, results in the growth of laterally extended voids in the Si substrate. The voids are loosely spaced and are of hexagonal shape, as seen in the plan-view image shown in Fig. 7(a). These voids are formed down to the buffer layer [Fig. 7(b)]. No porosity was found in the buffer layer, but faults and particles were found to decorate the original Si surface, as seen in Fig. 7(c). The form of the grain boundary regions lying between the SiC columns was investigated using HRTEM. Figure 7(d) shows an image of a grain boundary where amorphous material may be clearly seen, as at A.

Growth of the films under Si stabilized conditions for these growth parameters proceeds via three-

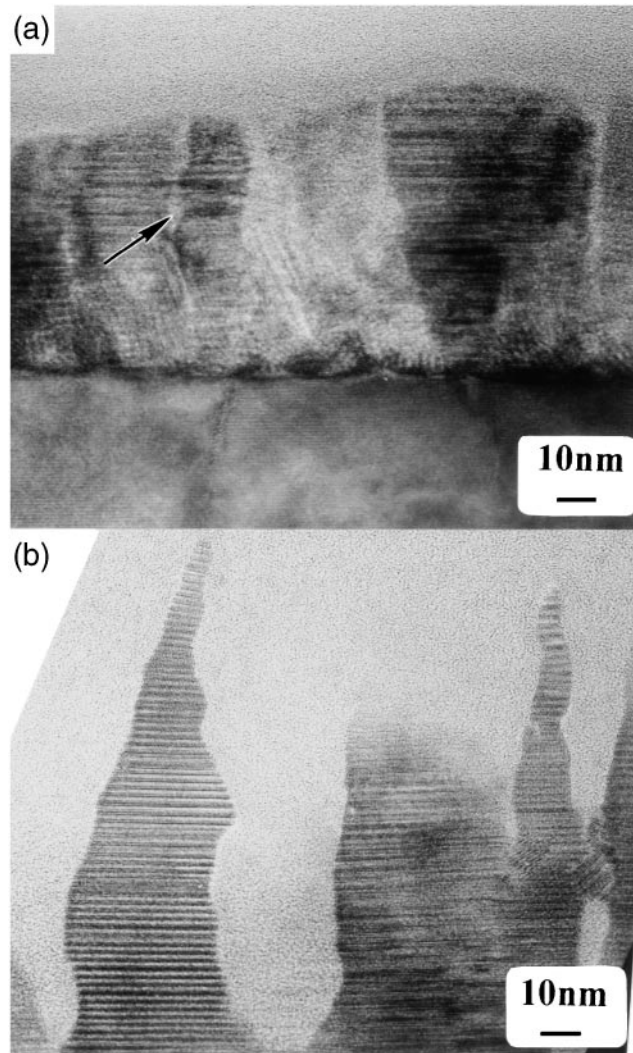


FIG. 6. High-resolution TEM image of specimen 5 showing (a) the intergranular amorphous zones and (b) the uppermost part of the SiC layer where the hexagonal polytype was formed.

dimensional nucleation. There is clear microstructural evidence that the process involves out-diffusion of Si from the substrate. For temperatures up to 800 °C, the diffusion results in the formation of pores in the substrate as compared with triangular-shaped voids above 800 °C and hexagonal-shaped voids when the specimen is annealed after initial growth. It has been proposed that a vacancy diffusion mechanism for Si exists at temperatures below 1270 °C.¹⁸ This process presumably results in the clustering of vacancies and the formation of the voids formed either during the interaction of two SiC islands¹⁹ or at the substrate defects.²⁰ Interestingly, the Si precipitates observed on the upper surface of the film are too large to have been formed by out-diffusion alone. Equally, they may not have been formed through the Si excess only. In contrast to the work of Diani *et al.*,²¹ no relationship has been found between the Si islands and

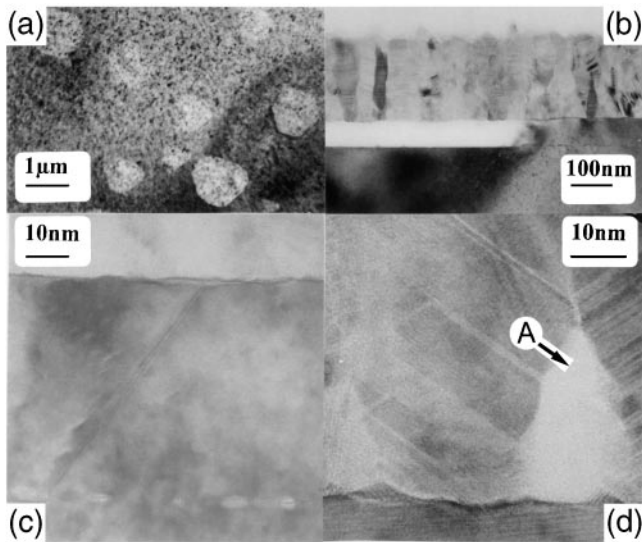
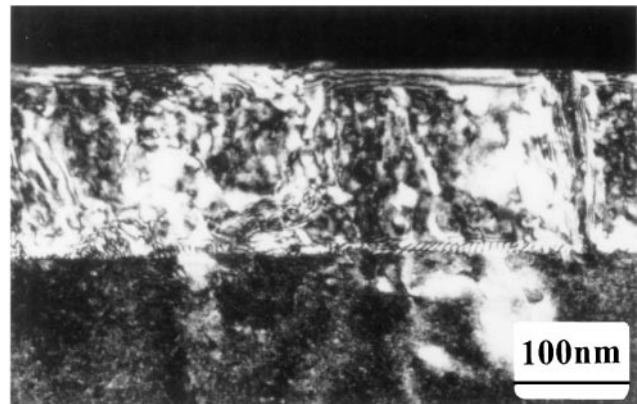


FIG. 7. TEM micrographs of specimen 6 as seen in (a) plan-view and (b), (c), and (d) cross section. Comparison of the micrographs shows that hexagonal-shaped voids have been formed in the substrate down to the buffer layer. An intergranular amorphous layer is marked at A in (d).

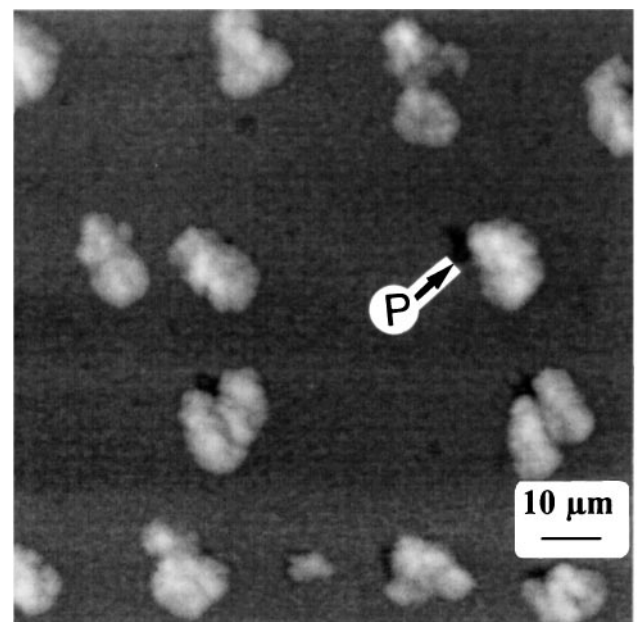
either the substrate voids or porous defects. However, the growth of SiC requires the homogeneous transport of Si to the growing surface. We assume that the diffusion driving force is the difference in the vapor pressure of Si within the voids and on the stabilized surface of the SiC. Thus, the diffusion path of Si seems to be the SiC grain boundaries. The lateral development of the grains being inhibited mostly likely by intergranular carbon deposits.

D. Film structure at 850–900 °C substrate temperature, low growth rate, and different adatom ratios

The effects of further reductions in the film growth rate have been investigated for overlayers formed at substrate temperatures of 850–900 °C, for which a clear relationship has been found between the flux rate ratio and epitaxial growth. Figure 8(a) is a dark-field micrograph of the film obtained using the 111 reflection, formed at 850 °C with an adatom ratio of Si : C of 1 : 1. The layer is cubic and contains different defects as well as boundaries. Such boundaries probably give rise to the step heights of ~ 1.5–3 nm observed in the AFM. While most of the surface of the film was found to be flat (but covered by few hexagonal shaped grains which are typically 1.5–10 nm in height), the AFM image shown in Fig. 8(b) indicates that many precipitates are located on the SiC surface, extending some 300 nm above the surface. Furthermore, the precipitates can be seen to be located at small triangular pits which have a typical depth of 10–55 nm. Although it is emphasized that voids were



(a)



(b)

FIG. 8. (a) Dark-field, cross-sectional TEM micrograph of specimen 6 obtained using 111 reflection of SiC and (b) an AFM image of the surface of the SiC film. The surface of the SiC is decorated with precipitates, which are associated with localized pit formation, as at P.

not observed in the TEM, the precipitates themselves were found to be single and polycrystalline Si.

In an attempt to control the formation of precipitates, depositions have been made using different adatom ratios. Three ratios have been investigated and these are referred to as Regions 1, 2, and 3 for which the adatom ratios were 0.95–1.01, 1.03–1.05, and 1.20–1.25, respectively (see Table I, specimen 7). The surfaces of the films formed in the different regions are shown in Figs. 9(a), 9(c), and 9(d). Figure 9(b) indicates the transitional growth between Regions 1 and 2 for an adatom ratio of between 1.01 and 1.03. These Normarski images show significant differences between the different

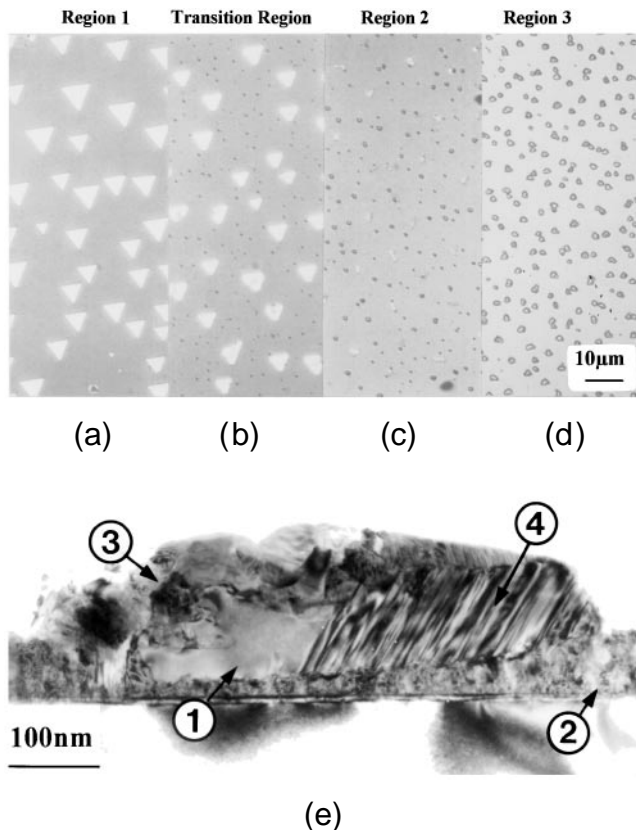


FIG. 9. Optical Normarski micrographs of the SiC films grown under adatom ratios of (a) 0.95...1.02 (region 1), (b) 1.02...1.05 (Transition Region), (c) app. 1.05 (Region 2), and (d) 1.20...1.25 (Region 3). (e) A bright-field micrograph of the SiC formed in Region 3 showing single crystalline Si (1), hexagonal SiC (4), and polycrystalline SiC (3) in a 3C SiC layer (2).

films. In Region 1, for example, a relatively high density of triangular features can be seen, while they were identified as voids with TEM, which are not apparent for Region 3. However, the grain size of the film in the latter region can be seen to be bimodal [Fig. 9(d)]. The large grains for this film were found to be SiC hillocks [see Fig. 9(e)] and the smaller grains to be Si which tended to be situated on top of the film. For the relatively narrow adatom range (Region 2), both the small grains and voids are difficult to distinguish. This thus emphasizes the morphological changes that are associated with Region 1. The films were investigated in further detail, and Fig. 10 shows both TEM images, obtained at $\langle 110 \rangle$ zone of Si, as seen in the diffraction patterns, and AFM images for the three different growth regimes. The films were epitaxial for each region, although for Regions 1 and 3 the overlays consisted of columnar grains containing both the cubic and hexagonal polytypes whereas in Region 2 the layer is cubic. However, there was a greater tendency for the grains to be twinned and faceted in Region 1 than in Region 3 and it is interesting to note that the AFM image of Region 1 shows elevations of hexagonal-shaped features for which the rms roughness was found to be 2.4 nm. By comparison, the surface formed in Region 2 is significantly flatter (rms roughness = 1.2 nm), whereas in Region 3 the roughness is again high (2.8 nm).

It has been found possible to obtain further control over the formation of surface precipitates through the use of the alternate deposition of Si and C, as controlled at an atomic level by RHEED intensity oscillations for a substrate temperature of 850 °C. Figures 11(a) and

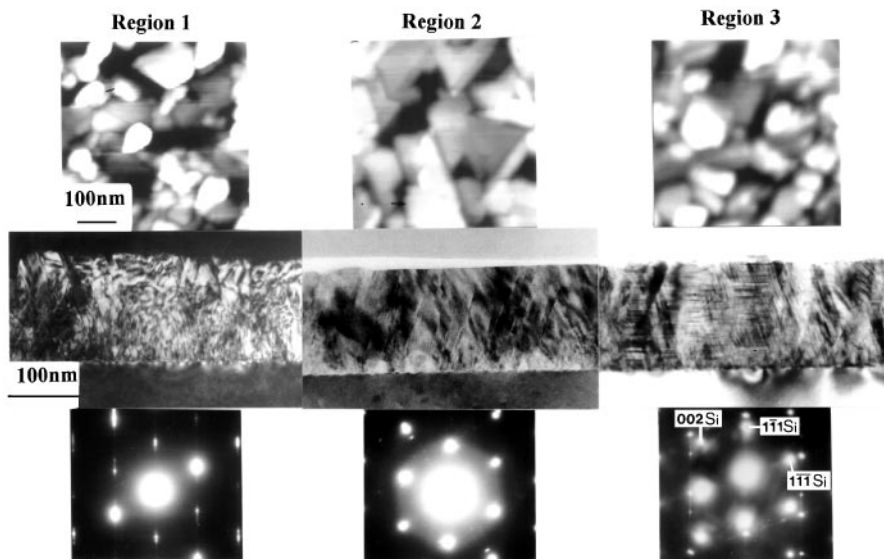


FIG. 10. AFM, TEM, and diffraction patterns of the SiC formed in Regions 1, 2, and 3. The AFM images show hexagonal-shaped elevations in Regions 1 and 3, but triangular shapes in Region 2. The diffraction patterns, obtained at the $\langle 110 \rangle$ zone of Si, show the presence of both the cubic and hexagonal polytypes in Regions 1 and 3 but only cubic polytype in Region 2, and this is confirmed by the morphologies seen in the bright-field TEM micrographs.

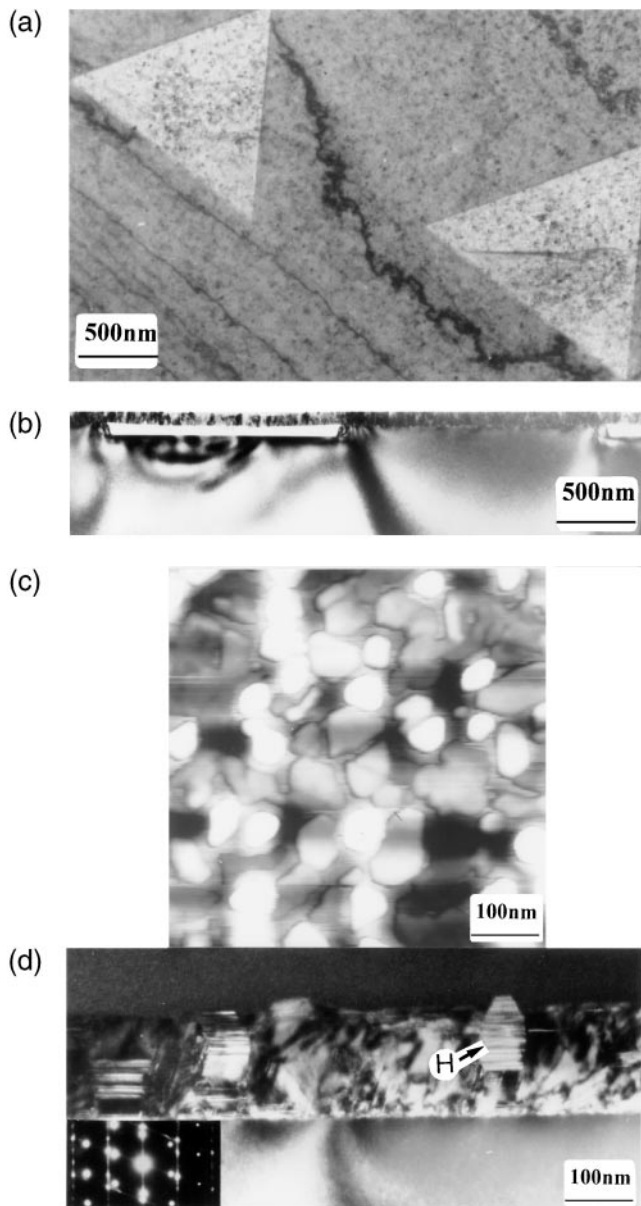


FIG. 11. The microstructure of the SiC film formed at 850 °C using alternate deposition of Si and C. Low magnification bright-field (a) plan-view and (b) cross-sectional TEM micrographs where coarse voids can be seen. Hexagonal-shaped grains are apparent in the AFM image in (c), and these features can also be observed at H in (d) which is a dark-field TEM micrograph. The inset diffraction pattern, obtained at [110] zone of Si, shows the presence of the cubic and hexagonal polytypes.

11(b) are bright-field TEM plan-view and cross-sectional micrographs, respectively, which demonstrate that no surface precipitates have been formed although large, characteristically shaped voids can be seen at the upper surface of the substrate. The films formed under these conditions were very flat (rms roughness = 1.0 nm), but had a tendency to form hexagonal-shaped elevations, as shown in Fig. 11(c). The microstructure of a typical

region of the film is shown in Fig. 11(d). The film consisted mainly of cubic SiC with a high stacking fault density, but was also found to include hexagonal SiC grains as labeled H (see also inset diffraction pattern, obtained at [110] zone of Si).

Our data have shown that the growth of single-crystal SiC films is promoted when the growth rate is reduced. The growth has been found to be very sensitive to the Si excess, so there is only a narrow range which results in the formation of high quality films, the volume fraction of surface Si precipitates, for example, increasing with adatom ratio. When the Si:C adatom ratio is as high as 1.25 the formation of extended hillocks occurs. These hillocks have a higher growth rate than the regions immediately surrounding them so that the consumption of Si is then locally increased and there is a tendency for the hillocks to be defective. When the growth takes place under conditions of low Si excess (< 1.1) both Si precipitates as well as voids are formed although such film features are excluded when the adatom ratio is reduced still further. This effect emphasizes our assumption that the out-diffusion of Si is caused by the difference in vapor pressure of Si within the voids and the growing Si-stabilized SiC surface. The morphological development of the films and their tendency toward the formation of voids can be compared to the layer deposited via the atomically controlled alternate supply of Si and C. Following the trends that have been described under conditions of alternate supply, void formation necessarily must occur simply because there is no Si excess. Extended voids were found and they do not contain polycrystalline SiC, as has also been found by Tin *et al.*²² It is assumed that they develop vertically through the Si buffer until the original Si surface is reached. At this point the rate of film growth rapidly falls and horizontal expansion of the voids occurs, as is consistent with our measurements which have shown that the volume of the voids is not a linear function of the layer thickness. The data described thus emphasize the fact that the voids are formed at an early stage of the film growth. Although our layers were grown on Si substrates of different oxygen content, the formation of voids was found not to be related to the oxygen content of the Si as was found by Leycuras.²³ It should thus be possible to avoid the formation of voids using alternate supply of Si and C only through the initial growth of a thin SiC buffer layer using a simultaneous supply of Si and C at a flux ratio of about 1.05 followed by the alternate deposition of Si and C.

IV. SUMMARY

The influence of different growth parameters on the microstructural development of SiC films grown by solid-source MBE has been described. Three distinct film

morphologies have been observed although the formation of epitaxial layers has been found to be promoted when the growth rate is low and for adatom Si:C ratios of 0.95 to 1.25. The boundaries of these adatom ratios were characterized by either the formation of voids in the substrate, surface Si precipitates, or SiC hillocks within the layers. When the deposition was carried out alternately from two sources, extended voiding was observed as well as the tendency for the formation of both cubic and hexagonal polytypes. Current work is addressing the problem of how to suppress the formation of defects and the results and how to promote the formation of hexagonal polytypes. The results of these investigations will be described in due course.

ACKNOWLEDGMENTS

The authors acknowledge the financial support of this research by the British-German ARC program (No. 313-ARC-VII), the Sonderforschungsbereich 196 (No. A03), German-Hungarian Intergovernmental Cooperation (No. 113), and the Newton Trust (Cambridge). We also thank Dr. Chrispin Hetherington for his help with the high resolution TEM.

REFERENCES

1. T. Nishino, J. A. Powell, and H. A. Will, *Appl. Phys. Lett.* **42**, 460 (1983).
2. H. Carter, R. F. Davis, and S. R. Nutt, *J. Mater. Res.* **1**, 811 (1986).
3. J. Steckl and J. P. Li, *Thin Solid Films* **216**, 144 (1992).
4. I. Kaneda, Y. Sakamoto, Ch. Nishi, M. Kanaya, and S-I. Hannai, *Jpn. J. Appl. Phys.* **25**, 1307 (1986).
5. I. Kaneda, Y. Sakamoto, T. Mihara, and T. Tanaka, *J. Cryst. Growth* **81**, 536 (1987).
6. L. Zou, Z. Ma, M. E. Lin, T. C. Shen, L. H. Allen, and H. Morkoc, *J. Cryst. Growth* **134**, 167 (1993).
7. A. Fissel, B. Schröter, and W. Richter, *Appl. Phys. Lett.* **66**, 3182 (1995).
8. D. Allendorf and D. A. Outka, *Surf. Sci.* **258**, 177 (1991).
9. J. Motayama, N. Morika, and S. Kaneda, *J. Cryst. Growth* **100**, 615 (1990).
10. A. Fissel, U. Kaiser, K. Pfennighaus, B. Schröter, and W. Richter, *J. Cryst. Growth* **154**, 72 (1995).
11. A. Fissel, U. Kaiser, K. Pfennighaus, B. Schröter, and W. Richter, *Appl. Phys. Lett.* **68**, 1204 (1996).
12. A. Fissel, B. Schröter, J. Kräußlich, and W. Richter, *Thin Solid Films* **238**, 64 (1995).
13. J. Kräußlich, A. Fissel, U. Kaiser, K. Goetz, and L. Dressler, *J. Appl. Phys. D* **28**, 759 (1995).
14. K. Pfennighaus, A. Fissel, U. Kaiser, M. Wendt, J. Kräußlich, G. Peiter, B. Schröter, and W. Richter, *Mater. Sci. Eng.* **B46**, 164 (1997).
15. T. Cheng and H. Aindow, *Philos. Mag. Lett.* **62**, 239 (1990).
16. J. D. Hetherington, U. Kaiser, S. B. Newcomb, and W. M. Stobbs, in *Inst. Phys. Conf. Vol. 147, Electron Microscopy and Analysis*, edited by D. Cherns (Institute of Physics, Bristol, 1995), p. 389.
17. W. Wahab, M. R. Sardela, J. Hultman, A. Henry, M. Willaner, E. Janzen, and J. E. Sundgen, *Appl. Phys. Lett.* **65**, 725 (1994).
18. J. Borg and G. J. Dienes, *An Introduction to Solid State Diffusion* (Academic Press, Boston, London, 1988).
19. P. Li and A. J. Steckl, *J. Electrochem. Soc.* **142**, 634 (1995).
20. P. Barna, *Phys. Scripta* **T49**, 349 (1993).
21. D. Diani, A. Mesli, L. Kubler, A. Claverie, J. L. Balladore, D. Aubel, S. Peyre, T. Heiser, and J. L. Bischoff, *Mater. Sci. Eng.* **B29**, 110 (1995).
22. C. Tin, R. Hu, R. L. Coston, and J. Park, *J. Cryst. Growth* **148**, 116 (1995).
23. L. Leycuras, *Appl. Phys. Lett.* **70**, 1533 (1997).